Behavioral/Cognitive

D_1-Dependent 4 Hz Oscillations and Ramping Activity in Rodent Medial Frontal Cortex during Interval Timing

Krystal L. Parker,[1] Kuan-Hua Chen,[1] Johnathan R. Kingyon,[1] James F. Cavanagh,[3] and Nandakumar S. Narayanan[1,2]

[1]Department of Neurology and [2]Aging Mind and Brain Initiative, Carver College of Medicine, University of Iowa, Iowa City, Iowa 52242, and [3]Department of Psychology, University of New Mexico, Albuquerque, New Mexico 87131

Organizing behavior in time is a fundamental process that is highly conserved across species. Here we study the neural basis of timing processes. First, we found that rodents had a burst of stimulus-triggered 4 Hz oscillations in the medial frontal cortex (MFC) during interval timing tasks. Second, rodents with focally disrupted MFC D_1 dopamine receptor (D1DR) signaling had impaired interval timing performance and weaker stimulus-triggered oscillations. Prior work has demonstrated that MFC neurons ramp during interval timing, suggesting that they underlie temporal integration. We found that MFC D1DR blockade strongly attenuated ramping activity of MFC neurons that correlated with behavior. These macro- and micro-level phenomena were linked, as we observed that MFC neurons with strong ramping activity tended to be coherent with stimulus-triggered 4 Hz oscillations, and this relationship was diminished with MFC D1DR blockade. These data provide evidence demonstrating how D1DR signaling controls the temporal organization of mammalian behavior.

Key words: **dopamine; interval timing; medial frontal cortex; Parkinson's disease**

Introduction

The ability to guide movements in time is a highly conserved mammalian behavior (Buhusi and Meck, 2005). On conscious reflection, this ability seems effortless. Yet this fundamental process is compromised in human diseases with altered dopamine signaling, such as attention deficit hyperactivity disorder (ADHD), schizophrenia, and Parkinson's disease (Malapani et al., 1998; Cools and D'Esposito, 2011; Parker et al., 2013b). Understanding the neural basis of timing could elucidate the nature of disease states and identify novel therapeutic targets.

Timing can be operationalized using an interval estimation task (Church, 1984; Gibbon et al., 1984). In this task, subjects estimate an epoch of several seconds (as indicated by a discriminative stimulus) by making a motor response after the interval has elapsed (Fig. 1). Interval timing can be studied in both rodents and humans (Rakitin et al., 1998; Balci et al., 2008). According to the scalar-expectancy theory, timed behavior involves a pacemaker-accumulator to estimate the passage of time, which is then compared with a memory for the temporal rule via a decision process (Church, 2003). Other theories of interval timing postulate different comparison processes, but all involve mechanisms to actively estimate the passage of time to inform response selection (Mauk and Buonomano, 2004; Simen et al., 2011).

Interval timing requires corticostriatal systems (Matell et al., 2003; Jahanshahi et al., 2010) including medial frontal cortex (MFC) and dorsal striatum (Coull et al., 2011). Inactivation of MFC in rodents profoundly impairs interval timing (Kim et al., 2009; Narayanan et al., 2012). Single MFC neurons are temporally modulated in humans, primates, and rodents (Niki and Watanabe, 1979; Narayanan and Laubach, 2009a; Sheth et al., 2012). MFC ramping activity, or activity that consistently increases or decreases with time, codes for interval duration and predicts when animals respond (Kim et al., 2013; Xu et al., 2014). Ramping activity is not specifically linked with movements (Narayanan and Laubach, 2009a; Kim et al., 2013). Rather, this ramping pattern has been posited to specifically encode time in a variety of tasks with temporal properties (Durstewitz, 2003).

Interval timing is influenced by dopamine. Amphetamine shifts responding forward in time (Taylor et al., 2007), whereas diseases with disrupted dopamine involve interval timing impairments attributable, in part, to dysfunctional temporal memories (Parker et al., 2013b). We previously demonstrated that blocking the D_1 (but not D_2) receptors within MFC impairs interval timing (Narayanan et al., 2012) and temporal processing during simple reaction time tasks (Parker et al., 2013a). These findings motivate the hypothesis that D_1 dopamine within the MFC is necessary for the ramping activity linked with temporal control.

In this study, we compared MFC single-neuron activity and local field potentials (LFPs) in rodents with and without MFC D_1 dopamine receptor (D1DR) blockade. We describe three novel results during interval timing tasks: (1) a burst of stimulus-triggered 4 Hz oscillations; (2) focal blockade of MFC D1DR

Received July 7, 2014; revised Oct. 27, 2014; accepted Oct. 31, 2014.

Author contributions: K.L.P., K.-H.C., J.R.K., J.F.C., and N.S.N. designed research; K.L.P., K.-H.C., and J.R.K. performed research; K.L.P., J.F.C., and N.S.N. analyzed data; K.L.P., K.-H.C., J.R.K., J.F.C., and N.S.N. wrote the paper.

This work was supported by NIH Grant K08 NS078100, NARSAD Young Investigator Awards to K.L.P. and N.S.N., and Nellie Ball Trust to K.L.P. We thank Mark Laubach for sharing software, for providing analysis tools for partial correlation analysis, and for comments on this manuscript. We thank Benjamin Land and Ralph DiLeone for comments on this manuscript and Adam D. Miller for technical assistance.

The authors declare no competing financial interests.

Correspondence should be addressed to Nandakumar S. Narayanan, 25 S. Grand Avenue, Medical Laboratories ML2110, Iowa City, IA 52242. E-mail: nandakumar-narayanan@uiowa.edu.

DOI:10.1523/JNEUROSCI.2772-14.2014

Copyright © 2014 the authors 0270-6474/14/3416774-10$15.00/0

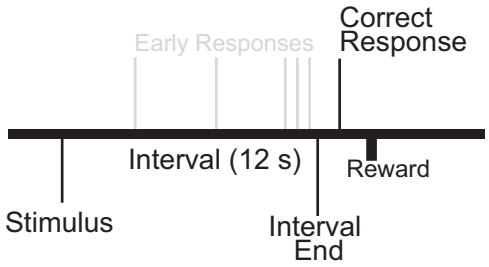

Figure 1. Interval timing task. Subjects estimate a 12 s interval starting with the onset of a discriminative stimulus by making a motor response; multiple responses per trial are permitted.

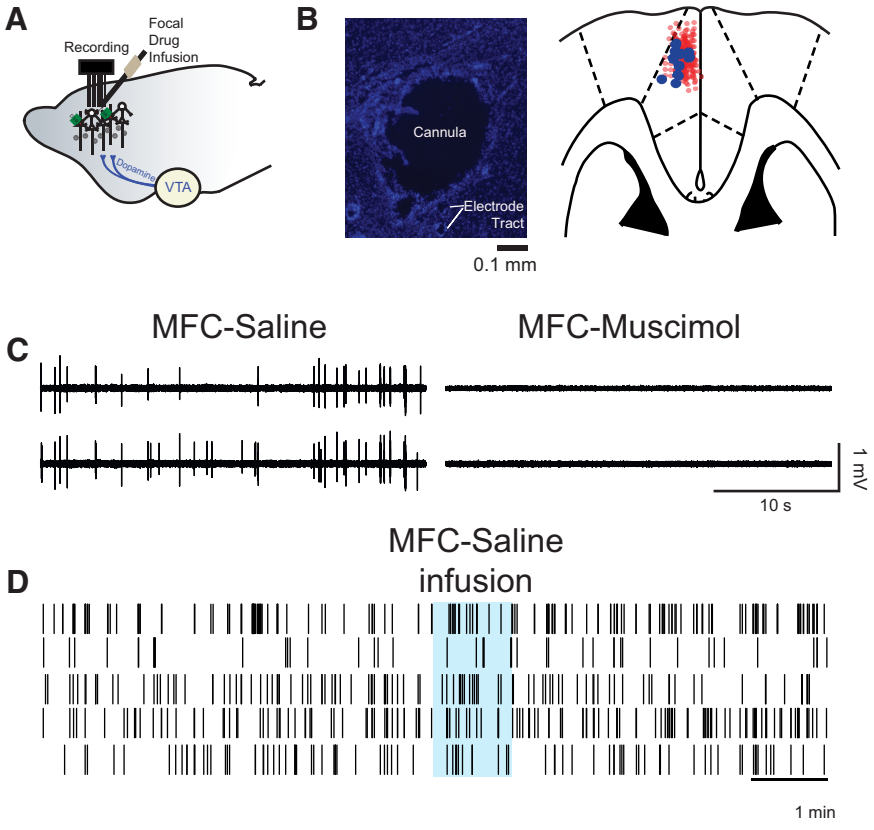

Figure 2. Medial frontal cortex (MFC) infusions. ***A***, We stereotaxically implanted cannula at a high angle to target recording electrodes in MFC. ***B***, Photomicrograph of a cannula tract and immediately neighboring electrodes (left; section stained with DAPI). Cannula locations were reconstructed from histological sections (right); the cannula is marked by blue circles, and electrode locations are marked by light red circles. ***C***, Wide band (unfiltered signal) from two electrodes in ***B*** showing single units in saline sessions and no spiking activity in sessions with muscimol infused into the MFC. Across 135 electrodes in nine animals, we could not identify any single units in sessions with muscimol infused into MFC. ***D***, Saline infusion did not change neural activity or our ability to isolate neurons during an acute recording session.

dopamine attenuates oscillations; and (3) focal MFC D_1 blockade decreases ramping activity linked with timing and coherent with 4 Hz oscillations. These data provide insight into how MFC dopamine signaling regulates the temporal organization of behavior.

Materials and Methods

Rodents. This study involved a total of nine male Long–Evans rats (aged 2 months; 200–225 g). Rats were trained to perform an interval timing task according to methods described previously (Narayanan et al., 2012). Animals were motivated by regulated access to water, whereas food was available *ad libitum*. Rats consumed 10–15 ml of water during each behavioral session, and additional water (5–10 ml) was provided 1–3 h after each behavioral session in the home cage. Single housing and a 12 h light/dark cycle were used; all experiments took place during the light cycle. Rats were maintained at ~90% of their free-access body weight during the course of these experiments and received 1 d of free access to water per week. All procedures were approved by the Animal Care and Use Committee at the University of Iowa.

Interval timing task. Rats were trained in interval timing tasks using standard operant procedures described in detail previously (Narayanan et al., 2012; Parker et al., 2013a). First, animals learned to make operant lever presses to receive liquid rewards. After fixed-ratio training, animals were trained in a 12 s fixed-interval timing task in which rewards were delivered for responses after a 12 s interval (Fig. 1). Rewarded presses were signaled by a click and an "off" house light. Each rewarded trial was followed by a 6, 8, 10, or 12 s pseudorandom intertrial interval that concluded with an "on" house light signaling the beginning of the next trial. Early responses occurring before 12 s were not reinforced. The house light was turned on at trial onset and lasted until the onset of the intertrial interval. Training and infusion sessions were 60 min long. Response time was defined as the average time the animals pressed the lever on each trial, which is typically used to estimate animals' internal estimates of time (Church, 2003; Caetano and Church, 2009; Narayanan et al., 2012).

Behavioral apparatus. Operant chambers (MED Associates) were equipped with a lever, a drinking tube, and a speaker driven to produce an 8 kHz tone at 72 dB. Behavioral arenas were housed in sound-attenuating chambers (MED Associates). Water rewards were delivered via a pump (MED Associates) connected to a standard metal drinking tube (AnCare) via Tygon tubing.

Rodent experimental protocol. Rats were first trained in the interval timing task and then implanted with a fixed microwire array and cannula into the MFC. After acclimatizing to recording procedures, a single manipulation-free session was recorded in the first five rats. This session was omitted in the final four rats. Then, all nine rats received a saline infusion into the MFC before neurophysiological recording. The very next day, they received an infusion of the D_1 receptor antagonist SCH23390 into the MFC. The next day, neurophysiological data were collected without any manipulation. Next, to check electrode placement, muscimol was infused into the MFC while neurophysiological data were recorded outside of the behavioral arena. Each rat had only one saline session and one MFC D1DR inactivation session on a separate day. Statistical comparisons between saline and MFC infusion sessions made no assumption that we recorded identical neurons in both sessions (Narayanan and Laubach, 2006, 2008; Narayanan et al., 2013). Some rodents were then run in unrelated pilot experiments (<2 weeks). Finally, animals were perfused.

Surgical and perfusion procedures. Rats trained in the 12 s interval timing task were implanted with a microwire array and a 33 gauge infusion cannula (Plastics One) in the medial frontal cortex according to procedures described previously (Narayanan and Laubach, 2006). Briefly, animals were anesthetized using ketamine (100 mg/kg) and xylazine (10 mg/kg). A surgical level of anesthesia was maintained with hourly (or as needed) ketamine supplements (10 mg/kg). Under aseptic surgical conditions, the scalp was retracted, and the skull was leveled between bregma and lambda. A single craniotomy was drilled over the area above the MFC, and four holes were drilled for skull screws. A

microelectrode array configured in 4 × 4 ($n = 2$) or 2 × 8 ($n = 7$) arrays of 50 μm stainless steel wires (250 μm between wires and rows; impedance measured *in vitro* at 400–600 kΩ; Plexon) were implanted in nine animals (coordinates from bregma: AP, +3.2; ML, ±1.2; DV, −3.5; at 12° in the lateral plane). Electrode ground wires were wrapped around the skull screws. The electrode array was inserted while concurrently recording neuronal activity to verify implantation in layer II/III of the MFC. The infusion cannula was then lowered to target the neurons being recorded (coordinates from bregma: AP, +0.3; ML, ±1.0; DV, −4.6; at 40° in the lateral plane; targeting bregma coordinates +3.2 AP, ±1.0 ML, −3.4 DV in the center of the recording array). Given past studies of diffusion volume, this approach suggested that drug infusions via these cannulae could modulate neural activity at these electrodes ~1.0 mm away (Myers, 1966; Martin and Ghez, 1993; Krupa et al., 2004; Allen et al., 2008). The craniotomy was sealed with cyanoacrylate (SloZap; Pacer Technologies) accelerated by ZipKicker (Pacer Technologies) and with methyl methacrylate (i.e., dental cement; A-M Systems). After implantation, animals recovered for 1 week before being reacclimatized to behavioral and recording procedures.

When experiments were complete, rats were anesthetized, overdosed with injections of 100 mg/kg sodium pentobarbital, and transcardially perfused with 10% formalin. Brains were postfixed in a solution of 10% formalin and 20% sucrose before being sectioned on a freezing microtome. Brain slices were mounted on gelatin-subbed slides and stained for cell bodies using DAPI. Histological reconstruction was completed using postmortem analysis of electrode and cannula placements and confocal microscopy in each animal. These data were used to determine electrode and cannula placement within the MFC.

To verify that our infusions did not induce neuronal displacement as a result of pressure from the bolus delivery, we performed an acute surgery involving MFC neuronal recordings during a saline infusion in one animal. Neuronal activity in the MFC was recorded for 3 min before a 0.5 μl infusion of saline and then for an additional 3 min involving the 1 min infusion and 2 min postinfusion.

MFC infusions. Focal drug infusions into MFC were performed according to procedures described previously (Narayanan and Laubach, 2006; Narayanan et al., 2006, 2013; Allen et al., 2008). One week after surgery, animals were lightly anesthetized with isoflurane via a nosecone for 5 min, recording cables were attached, and the animal was allowed to recover for 30 min before being tested in the interval timing task. On subsequent days, the MFC was infused with either 0.9% saline (Phoenix Scientific) during control sessions or D_1 dopamine antagonist SCH23390 (0.5 μg of 1.0 μg/μl; Sawaguchi and Goldman-Rakic, 1994; Narayanan et al., 2012; Parker et al., 2013a) while anesthetized via isoflurane. Infusion was conducted by inserting an injector into the guide cannula, and 0.5 μl of infusion fluid was delivered at a rate of 30 μl/h (0.5 μl/min) via a syringe infusion pump (KD Scientific). After the injection was complete, the injector was left in place for 2 min to allow for diffusion. To confirm that drug infusion modulated neuronal activity from nearby recording arrays, 0.5 μg of muscimol (1.0 μg/μl; Allen et al., 2008), a $GABA_A$ receptor agonist (Sigma-Aldrich), was infused into MFC. After 30 min, all channels in all animals had complete silencing of neural activity after muscimol infusions at all recording sites; we were not able to isolate any neurons from 135 electrodes in nine animals after muscimol infusion (Fig. 2). Additionally, the pressure of the bolus did not influence neuronal firing as shown by saline infusion during acute recordings (Fig. 2*D*).

Neurophysiological recordings. Neuronal ensemble recordings in the MFC were made using a multielectrode recording system (Plexon). Putative single neuronal units were identified on-line using an oscilloscope and audio monitor. The Plexon off-line sorter was used to analyze the signals after the experiments and to remove artifacts. Spike activity was analyzed for all cells that fired at rates above 0.1 Hz. Statistical summaries were based on all recorded neurons. No subpopulations were selected or filtered out of the neuron database. The LFP was recorded using wideband boards with bandpass filters between 0.07 and 8000 Hz. Principal component analysis (PCA) and waveform shape were used for spike sorting. Single units were identified as having (1) consistent waveform shape, (2) separable clusters in PCA space, (3) a consistent refractory period of at least 2 ms in interspike interval histograms, and (4) consistent firing rates around behavioral events (as measured by a runs test of firing rates across trials around behavioral events; neurons with $|z|$ scores >4 were considered "nonstationary" and were excluded). Analysis of neuronal activity and quantitative analysis of basic firing properties were performed using NeuroExplorer (Nex Technologies) and with custom routines for MATLAB. Peri-event rasters and average histograms were constructed around light on, lever release, lever press, and lick. Microwire electrode arrays comprised 16 electrodes. In each animal, one electrode without single units was reserved for local referencing, yielding 15 electrodes per rat. LFPs were recorded from four of these electrodes per rodent. LFP channels were analog filtered between 0.7 and 100 Hz on-line and recorded in parallel with single-unit channels using a wideband board. Consistent with our prior work, although examples of individual neurons are shown under different drug conditions (control and MFC D1DR blockade), our statistical analyses assume that these populations of neurons are independent (Narayanan and Laubach, 2006, 2008; Narayanan et al., 2013).

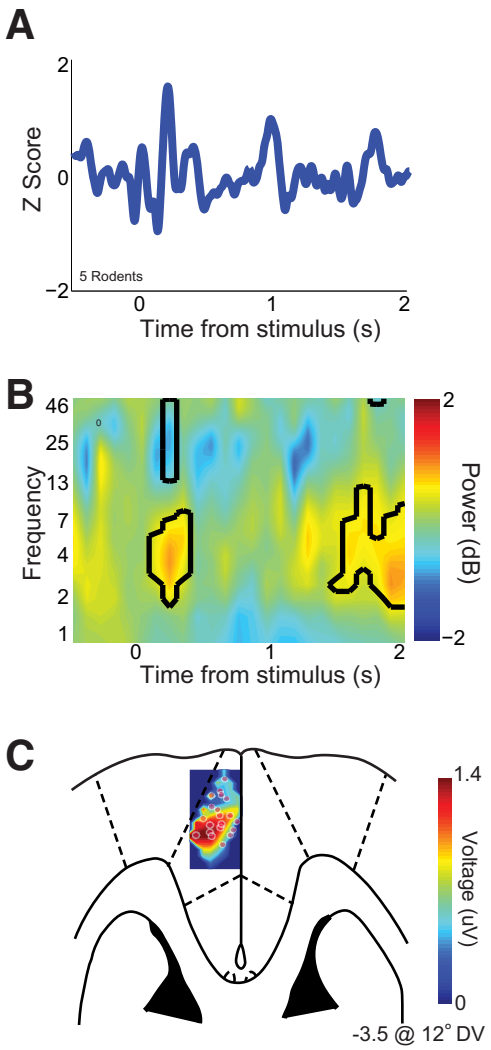

Figure 3. Interval timing involves stimulus-triggered 4 Hz oscillations. ***A***, Event-related potentials from all LFP channels in five rodents (20 channels) revealed a stimulus-triggered peak ~160 ms after stimulus onset. ***B***, Time–frequency analysis of signals revealed a prominent burst of low-frequency oscillations (~3–7 Hz) in rodent MFC LFPs. Black lines indicate changes in power relative to baseline at $p < 0.05$. ***C***, Voltage topography of stimulus-related ERPs revealed a prominent voltage source in MFC at approximately +3.0 mm AP and −3.5 DV from bregma.

We defined ramping activity as firing rate that progressed uniformly over the interval. We measured this in two ways: PCA and linear regression. PCA was used to identify dominant patterns of neuronal activity

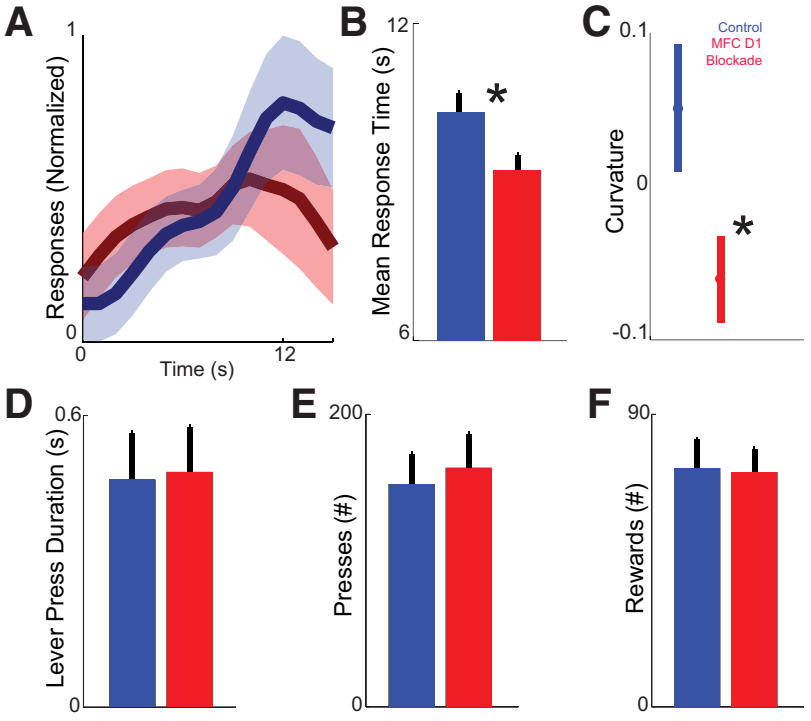

Figure 4. Medial frontal cortex (MFC) D1DR blockade impairs timing without changing other aspects of behavior. ***A***, The timing of responses (i.e., when animals pressed the lever) during interval timing for control sessions (blue) versus MFC D1DR blockade sessions (red) in nine animals. ***B***, Average response time was shorter in sessions with MFC D1DR blockade (red) compared with control (blue). $*p < 0.05$. ***C***, Curvature indices of time–response histograms were less in MFC D1DR sessions (blue) compared with control sessions. $*p < 0.05$. ***D–F***, MFC D1DR blockade did not change the duration of lever press (i.e., time the lever was held down; ***D***), the number of overall lever presses (***E***), or the number of overall rewards (***F***). Additionally, MFC D1DR blockade did not consistently change open-field behavior or other gross motor parameters. All plots are of mean ± SEM.

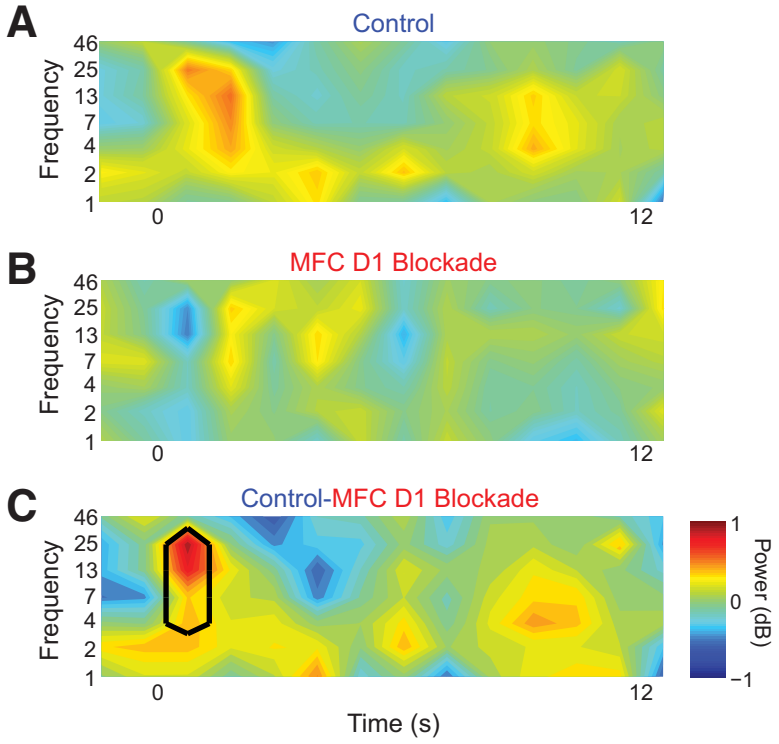

Figure 5. Medial frontal cortex (MFC) D1DR blockade attenuates stimulus-related 4–30 Hz oscillations. ***A***, In control sessions, a 3–25 Hz burst of oscillations occurred for ~2 s triggered by the onset of the stimulus at time 0. ***B***, In sessions with MFC D1DR blockade, this burst was not apparent. ***C***, Comparison subtraction of control minus MFC D1DR blockade sessions reveals more low-frequency power in control sessions only after stimulus onset between ~3–30 Hz. Black lines indicate $p < 0.05$. These data are from 30 MFC LFPs in nine rodents.

using orthogonal basis functions from peri-event histograms during the 12 s interval (Paz et al., 2005; Narayanan and Laubach, 2009a,b; Bekolay et al., 2014). All neurons from nine animals per session (control and MFC D1DR sessions) were included in PCA. The same principal components were projected onto control and MFC D1DR blockade sessions, and the weights were compared via a *t* test (Chapin and Nicolelis, 1999; Narayanan and Laubach, 2009b). Second, we used linear regression to define neuronal ramping activity. Ramping neurons are described as those with a significant relationship in a linear regression model (Kim et al., 2013).

Partial correlation analysis (MATLAB function partialcorr) was used to explore the relationship of spiking activity to prior outcome and response time using Spearman's nonparametric rank correlation (Narayanan et al., 2013). Response time was defined by the average time the animals pressed the lever on each trial and is typically used to estimate animals' internal estimate of time (Church, 2003; Caetano and Church, 2009; Narayanan et al., 2012). If the animal made multiple presses on a single trial, response times were averaged. In this analysis, response time was treated as a continuous variable. To visualize response times, peri-event rasters were sorted and quantitatively divided into tertiles by response times. This analysis partials out the influence of spike count or low-frequency amplitude computed via the Hilbert transform using a 100 ms sliding window starting at stimulus onset (code shared by personal communication with Mark Laubach). Statistical significance was assessed by shuffling trial orders 1000 times, and effect size was quantified using the absolute value of Spearman's rho statistic.

Time–frequency and neuronal analyses. Time–frequency calculations were computed using custom-written Matlab routines (Cavanagh et al., 2009). Time–frequency measures were computed by multiplying the fast Fourier transformed (FFT) power spectrum of LFP data with the FFT power spectrum of a set of complex Morlet wavelets [defined as a Gaussian-windowed complex sine wave: $e^{i2\pi tf}\, e^{-\frac{t^2}{2\times\sigma^2}}$, where t is time and f is frequency (which increased from 1 to 50 Hz in 50 logarithmically spaced steps), and defines the width (or "cycles") of each frequency band, set according to $4/(2\pi f)$], and taking the inverse FFT. The end result of this process is identical to time-domain signal convolution, and it resulted in the following: (1) estimates of instantaneous power (the magnitude of the analytic signal) defined as $Z[t]$ [power time series: $p(t) = \text{real}[z(t)]^2 + \text{imag}[z(t)]^2$]; and (2) phase (the phase angle) defined as arctan(imag$[z(t)]$/real$[z(t)]$). Each epoch was then cut in length surrounding the event of interest (−500 to +2000 ms). Power was normalized by conversion to a decibel scale [10*log10 [power(t)/power(baseline)]] from a prestimulus baseline of −500 to −300 ms, allowing a direct comparison of effects across frequency

bands. Statistical significance against the baseline was computed via a paired t test and is indicated by contours in the time–frequency plots, with a minimum threshold cluster size corresponding to 0.1 s by 2 Hz. To correct for multiple comparisons, empirical p values <0.05 were calculated based on 10^7 permutations of time–frequency plots (Narayanan et al., 2013).

To look at the time–frequency component of interactions between individual spikes and the field potential, we applied spike-field coherence analysis using the Neurospec toolbox (Rosenberg et al., 1989), in which multivariate Fourier analysis was used to extract phase-locking among spike trains and local field potentials. Phase-locking coherence values varied from 0 to 1, where 0 indicates no coherence and 1 indicates perfect coherence. Trial numbers were matched between animals and controls and MFC D1DR blockade sessions to ensure consistency of coherence measures. Statistical significance with multiple comparisons corrections was performed using spatial thresholding and permutations as above.

Results

Interval timing involves stimulus-triggered low-frequency oscillations in MFC

To study how MFC is involved in interval timing, we recorded neural activity from rodents performing an interval timing task (Fig. 1). In five rodents, stimulus-related potentials recapitulated canonical events in the event-related potential (ERP), including a large phase-locked oscillation after the stimulus onset (20 LFP channels from five rodents; this analysis includes all recorded channels; Fig. 3*A*). Spectral analysis revealed that this initial stimulus-related signal was accompanied by a burst of low-frequency power in the theta band (~4–8 Hz), with decreased beta band power (~12–30 Hz; Fig. 3*B*). ERP voltage topography was strongest at midfrontal LFP channels approximately +3.0 mm from bregma (Fig. 3*C*). These data suggest low-frequency oscillations in the theta range are involved in interval timing (Cavanagh et al., 2009, 2012; Narayanan et al., 2013).

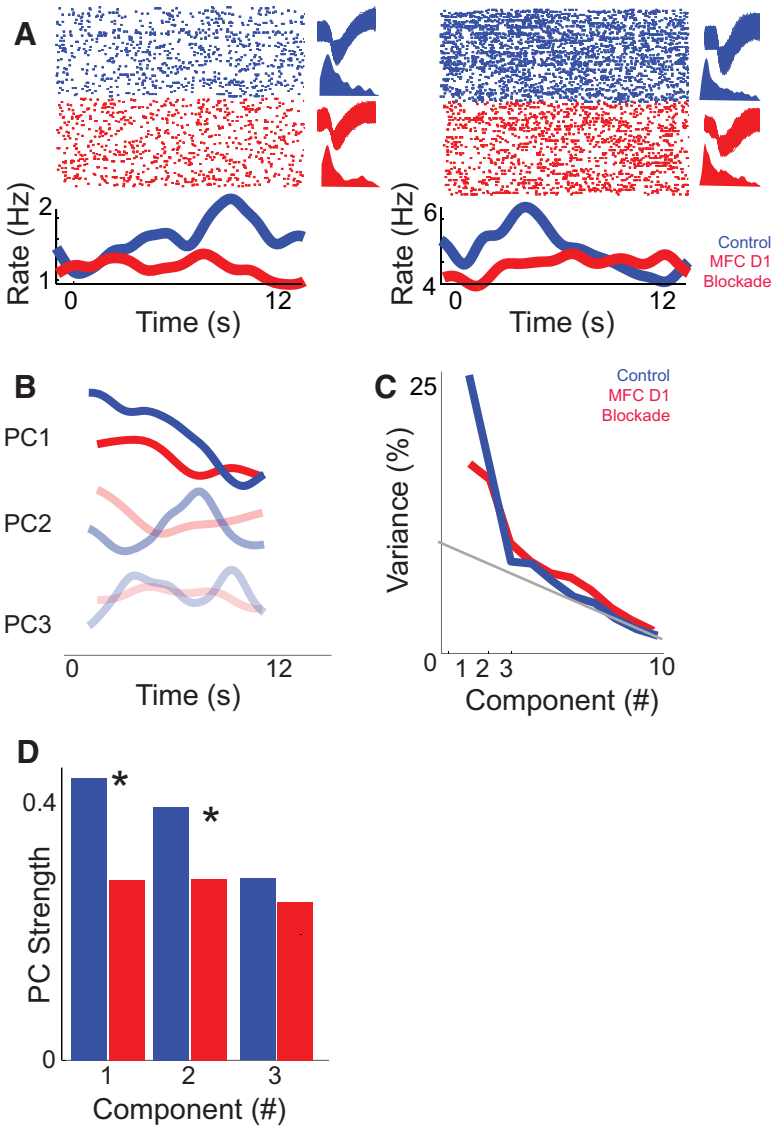

Figure 6. Medial frontal cortex (MFC) D1DR blockade decreases ramping activity. ***A***, Examples of MFC ramping neurons recorded in control (blue) sessions. In red, the same putative neuron from the control session is shown in MFC D1DR blockade sessions (red). These neurons were identified based on similar waveforms (top right) and interspike intervals (bottom right) in each condition. Note that these are two exemplars. The raster plot at the top shows neuronal activity as each dot represents an action potential (top); each row is a trial. The bottom line plot displays the average firing rates over time. Statistical comparisons assumed that independent populations were recorded in control and D1DR blockade sessions. ***B***, ***C***, Principal component analysis in control sessions (blue) revealed that ramping activity was the most prominent pattern of neural activity among MFC neurons (PC1; ***B***) and explained 27% of variance (***C***). In MFC D1DR sessions (red), a consistent ramping component was not observed, and PC1 explained less variance. ***D***, To directly compare ramping activity, we projected PCs from control sessions onto MFC D1DR sessions. PC1 explained significantly less variance in MFC D1DR blockade sessions, whereas PC3 was unchanged. Asterisks represent significance at $p < 0.05$ via a t test. Together, these data suggest that focal D1DR blockade attenuates ramping activity of neurons in MFC.

MFC D1DR blockade alters interval timing without changing motor behavior

Our prior work demonstrated that blocking D_1 dopamine signaling in the MFC with SCH23390 impairs interval timing (Narayanan et al., 2012). In this study, MFC D1DR blockade with 0.5 μl of 1 μg/μl SCH23390 impaired temporal control of responding in nine rodents, i.e., rodents in the D1DR blockade condition responded earlier than in control sessions (mean ± SEM response times per trial: control, 10.2 ± 0.3 s vs SCH23390, 9.2 ± 0.2 s; $t_{(8)} = 2.5$, $p < 0.04$; Fig. 4*A*,*B*).

We also measured interval timing performance using a curvature index that increases as animals' responses are guided by time during interval timing tasks (Fry et al., 1960). This index measures the deviation from the cumulative response record of a straight line. The curvature index has been used as a measure of temporal control during interval timing tasks that is independent of overall response rate, because animals' curvature indices increase as responses are controlled in time (Caetano and Church, 2009; Narayanan et al., 2012). Curvature indexes were significantly less in MFC D1DR sessions (0.05 ± 0.04 in control sessions vs −0.6 ± 0.03 MFC D1DR sessions; $t_{(8)} = 2.5$, $p < 0.04$; Fig. 4*C*).

Moreover, lever-pressing behavior was unchanged (duration of lever depression: 0.47 ± 0.01 vs 0.48 ± 0.01 s; $t_{(8)} = 0.33$, $p <$

0.75; Fig. 4*D*). Animals did not change overall responding or reward acquisition (total lever presses: 152 ± 20 vs 163 ± 33 lever presses in SCH23390 sessions, $t_{(8)} = 0.4$, $p < 0.67$; total rewards: 73 ± 9 vs 72 ± 7 lever presses in SCH23390 sessions, $t_{(8)} = 0.1$, $p < 0.92$; Fig. 4*E*,*F*). These data are consistent with our previous work demonstrating that MFC D_1 blockade specifically influences the timing of movements without influencing reward acquisition, general activity, or motor parameters (Narayanan et al., 2012; Parker et al., 2013a).

MFC D1DR blockade attenuates 4–30 Hz oscillations

We examined how MFC oscillations are influenced by MFC D1DR blockade. As in control sessions with vehicle infused into MFC (Fig. 2*B*), we observed a large burst of low-frequency oscillations (4–30 Hz) immediately after the stimulus, lasting ~2 s (Fig. 5*A*). However, with MFC D1DR blockade, this burst of oscillations was not prominent (Fig. 5*B*). A direct comparison of LFP power between control and SCH23390 sessions revealed significantly less 4–30 Hz power in sessions with MFC D1DR blockade ($p < 0.05$; Fig. 5*C*). These results showed that MFC D1DR blockade attenuates stimulus-related MFC low-frequency oscillations (Table 1).

MFC D1DR blockade decreases ramping activity

Ramping activities of MFC neurons have been proposed to encode time (Niki and Watanabe, 1979; Durstewitz, 2003; Narayanan and Laubach, 2009a; Kim et al., 2013; Xu et al., 2014). We recorded neuronal ensembles in MFC to test the hypothesis that MFC D1DR dopamine blockade decreases ramping activity and to investigate how ramping activity is related to MFC oscillations. We isolated 99 neurons from nine rats in saline sessions (0.7 neurons/electrode; 11.0 ± 4.6 neurons per rodent) and 91 neurons from the same rats in MFC D1DR blockade sessions [0.7 neurons/electrode or 10.1 ± 5.3 neurons per rodent; these numbers are in line with our previous work (Narayanan and Laubach, 2006, 2008, 2009a]. Also similar to our prior work, although we report individual neuron examples under different drug conditions, we recorded these neuronal populations on different days, and our statistical analyses assumed that these populations of neurons are independent (Narayanan and Laubach, 2006, 2008; Narayanan et al., 2013).

Ramping activity was defined as the firing rate that progressed uniformly over the interval. We measured this in two ways: PCA and linear regression. PCA identifies dominant patterns of neural activity using a data-driven approach. This technique identifies orthogonal basis functions, or prominent patterns of activity within a dataset without making prior assumptions (Narayanan and Laubach, 2009b). This technique has been used extensively in the past to quantify ramping activity (Narayanan and Laubach, 2009a; Bekolay et al., 2014). Similar to these prior studies, we found that the first component (PC1) ramped, or changed, its activity uniformly with time (Fig. 6*A*,*B*). Ramping activity was PC1 in seven of nine animals in control sessions. PC1 activity explained 27% of variance in our data (Fig. 6*C*). A second component (PC2) explained 17% of variance. These components appeared highly similar to those previously found from MFC neurons during the delay period in a simple reaction time task (Narayanan and Laubach, 2009a; Bekolay et al., 2014). They also matched ramping patterns of activity observed during interval timing tasks as well as other goal-directed tasks (Hyman et al., 2012; Ma et al., 2014). Smaller components explained progressively less variance (Fig. 6*C*). No ramping components were observed in MFC D1DR sessions. If MFC D1DR signaling influenced ramping activity, then ramping components should have less weight in MFC D1DR blockade sessions. To do this, we projected components from control sessions onto MFC D1DR sessions (Chapin and Nicolelis, 1999; Narayanan and Laubach, 2009b). Indeed, we found that PC1 was markedly weaker in MFC D1DR blockade sessions (PC1: $t_{(188)} = 3.3$, $p < 0.001$). Notably, PC2 was also weaker in MFC D1DR blockade sessions (PC2: $t_{(188)} = 3.0$, $p < 0.003$; Fig. 6*D*). Furthermore, MFC D1DR blockade did not change nonramping components such as PC3 (PC3: $t_{(188)} = 1.1$, $p < 0.26$; Fig. 6*D*). Finally, we used regression to analyze ramping activity. This analysis found that significantly fewer neurons fit a linear regression model in MFC D1DR sessions (11 neurons in control sessions vs 2 neurons in MFC D1DR sessions; $\chi^2 = 4.6$, $p < 0.03$). Notably, very few neurons were significantly fit via a log-based linear regression model, precluding further analysis of this model (three neurons in control sessions vs one neuron in MFC D1DR sessions). These data provide evidence that MFC D1DR blockade decreased ramping activity.

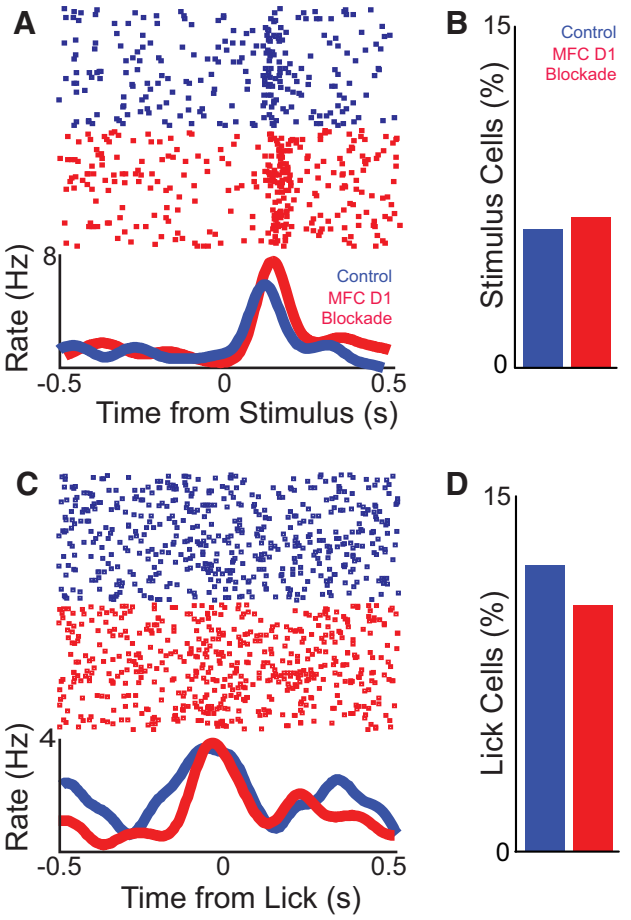

Figure 7. Medial frontal cortex (MFC) D1DR blockade does not change task-related modulations. ***A***, A putative neuron in control and D1DR blockade sessions showed identical stimulus-onset modulations. As in Figure 6, these are exemplars, and statistical comparisons assumed that independent populations were recorded in control and D1DR blockade sessions. The top portion displays the activity of a single neuron, and each dot represents an action potential; each row is a trial. The bottom line plot displays the average firing rates over time. ***B***, A similar fraction of neurons were stimulus onset modulated in control and MFC D1DR blockade sessions, as computed via a paired *t* test of firing rate 100 ms before/after stimulus onset; note the different time scale compared with Figure 6*A*. ***C***, A single putative neuron in control and D1DR blockade sessions showed similar lick-related modulation, as computed via a paired *t* test of firing rate 100 ms before/after lick. ***D***, The percentage of lick-modulated cells was also similar in control and MFC D1DR blockade sessions. Significance was determined at a level of $p < 0.05$.

Notably, MFC D1DR blockade did not change overall task modulation (measured by comparing the firing rate over the interval vs the intertrial interval via a paired t test; 27 of 99 in control vs 28 of 91 in MFC D1DR blockade sessions; $\chi^2 = 0.3$, $p < 0.6$). Moreover, MFC D1DR blockade did not change the overall firing rate (12 ± 2.5 spikes/s in control sessions vs 14.3 ± 4.3 spikes/s in MFC D1DR blockade sessions; $t_{(188)} = 0.45, p < 0.46$). MFC neurons had identical stimulus-related patterns of modulation in control and MFC D1DR blockade sessions (Fig. 7*A*), and a similar fraction of neurons were modulated around the stimulus (100 ms before/after around the light stimulus via a paired t test): six neurons in both control and MFC D1DR blockade were modulated (6% in control vs 6.6% in MFC D_1 blockade sessions; $\chi^2 = 0.02, p < 0.88$; Fig. 7*B*). MFC neurons also had identical lick-related patterns of modulation in control and MFC D1DR blockade sessions, and a similar fraction of neurons were modulated around licking (100 ms before/after time from lick via a paired t test; 12 vs 10%; control vs MFC D1DR blockade sessions; $\chi^2 = 0.24$, $p < 0.62$; Fig. 7*C*,*D*).

In summary, MFC D1DR blockade with SCH23390 did not change the number of neurons we were able to isolate, overall neuronal firing rate, stimulus-related modulation, licked-related modulation, or overall modulation. On the other hand, ramping activity was decreased in MFC D1DR blockade sessions. Together, these analyses suggest that MFC D1DR blockade decreases ramping activity of neurons without affecting other features of MFC neuronal modulation during interval timing.

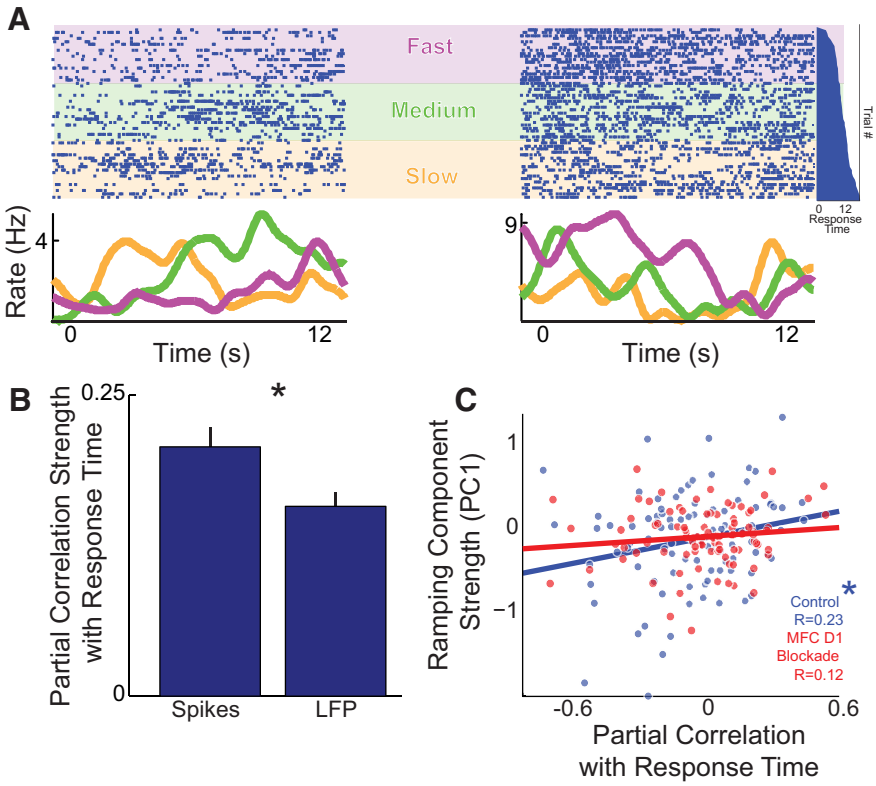

Figure 8. Ramping neurons can correlate with response times on each trial. ***A***, Two simultaneously recorded ramping MFC neurons from the same animal fired differently on trials with slow, medium, and fast tertiles of average response times. The top portion displays the activity of two single neurons, and each dot represents an action potential; each row is a trial. The bottom line plot displays the average firing rates over time. The vertical histogram (far right in dark blue) shows response times sorted on a trial-by-trial basis; trials on the top have short response times, and trials on the bottom have long response times, aligned with raster. Purple, "fast" third of response times; green, "medium," or middle third, of response times; orange, "slow" third of response times. Note that subsequent analyses treat the response time as a continuous variable. ***B***, Partial correlation across time with spikes and LFP revealed that spiking activity was more correlated with the response time. Data include all neurons and LFP channels in control sessions; 0–6 s epoch used for correlation to avoid motor confounds. Mean ± SEM plotted; $^*p < 0.05$. ***C***, In control sessions, neurons with strong positive ramping (PC1) were significantly positively correlated with response times ($n = 99$ neurons) and nonsignificantly correlated in MFC D1DR blockade ($n = 91$ neurons). $^*p < 0.05$.

Ramping neurons had very different firing rates as a function of response times, or the average time the animal pressed the lever on each trial. For instance, two simultaneously recorded MFC neurons with ramping activity had distinct firing patterns for the first tertile of response times (Fig. 8A; labeled 'slow' in orange), for the middle tertile of response times (labeled "medium," in green), and for the last tertile of response times (labeled "fast," in purple). To determine whether ramping activity or low-frequency oscillations were more predictive of animals' internal estimates of time, we used partial correlation analysis (Narayanan et al., 2013). This technique performs a linear correlation between two variables controlling for variance in a third variable. In this case, we were interested in whether the amplitude of low-frequency oscillations (Figs. 2, 5; amplitude computed by a Hilbert transform of 1–12 Hz oscillations of LFP) or ramping activity (Fig. 6) were more predictive of animals' response times. To avoid motor confounds, we restricted our analysis to the part of the interval when the animal was least likely to respond (the first 0–6 s of the interval). Results showed that partial correlation strength for ramping activity was stronger than for low-frequency oscillation amplitude (|Partial correlation| corresponding to strength: for spikes, 0.21 ± 0.02; for LFP, 0.16 ± 0.0; paired $t_{(98)} = 3.2, p < 0.002$; Fig. 8*B*) and significantly stronger than trial-shuffled noise (based on shuffling trial order 10^7 times for each neuron; paired $t_{(98)} = 2.9, p < 0.005$).

Ramping activity computed by PCA was positively correlated with partial correlation of neuronal activity (PC1 vs partial correlation: $r = 0.23, t_{(97)} = 2.3, p < 0.01$; Fig. 8*C*). That is, neurons that ramped down over the interval fired more on trials with long response times, and neurons that ramped up over the interval fired more on trials with short response times (see Fig. 8*A* for examples). As reported above, ramping components were diminished in sessions with MFC D1DR blockade, and ramping component strength was no longer significantly related to mean response time ($r = 0.12, t_{(89)} = 1.1, p < 0.13$), although Fisher's r to z test suggested that correlations in control sessions were not significantly larger than the MFC D1DR blockade session ($Z = 0.8, p < 0.22$). These data indicate that ramping neuronal activity is more predictive of animals' internal estimates of time than the local field potential. This is broadly consistent with prior evidence suggesting that ramping activity among single neurons is predictive of when animals respond during interval timing (Kim et al., 2013; Xu et al., 2014).

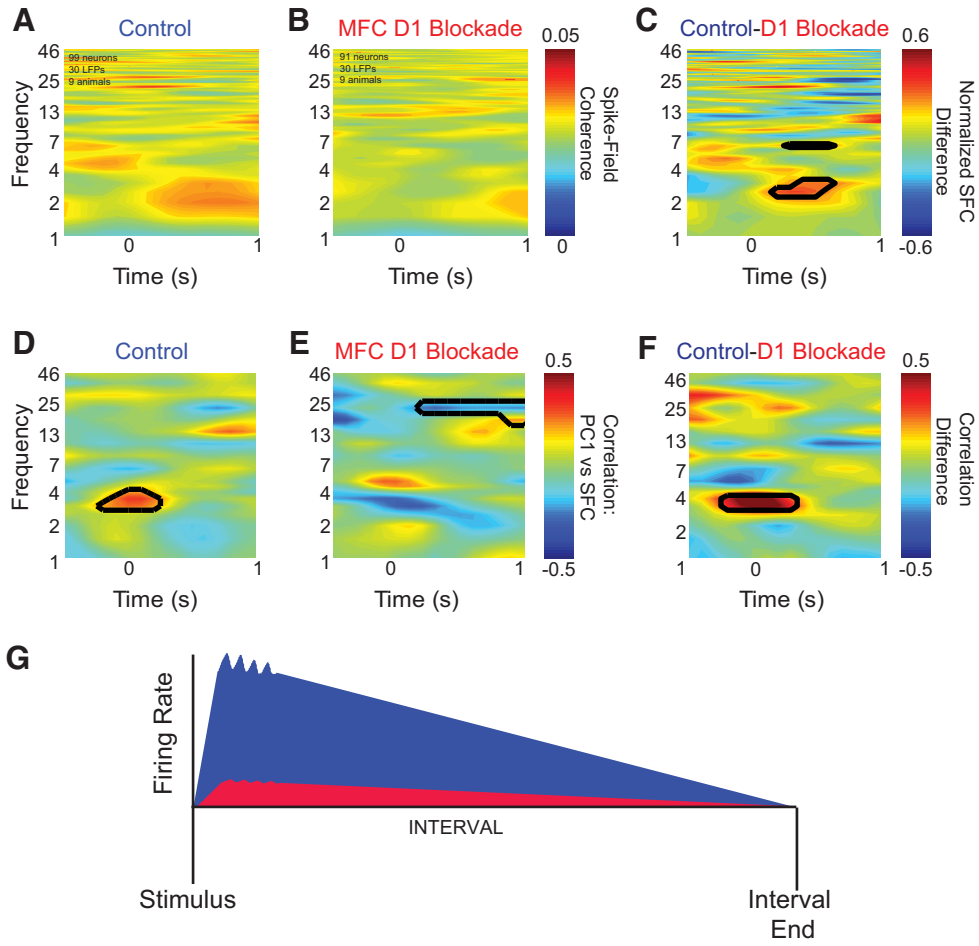

Figure 9. Medial frontal cortex (MFC) D1DR blockade eliminates ~4 Hz spike-field coherence. ***A***, ***B***, Across all nine animals (99 MFC neurons and 30 LFP channels), weak spike-field coherence was observed after stimulus onset in control sessions (***A***) but not in MFC D1DR blockade sessions (91 MFC neurons and 30 LFP channels; ***B***). ***C***, Subtracting the two revealed significant differences in functional coupling in low frequencies (~2–4 and 7 Hz) after stimulus onset. The scale is normalized; black lines indicate significance at $p < 0.05$. ***D***, ***E***, To test whether neurons with ramping activity tended to have spike-field coherence (SFC), we explored the relationship of PC1 with spike-field coherence and found significant correlations between 3–5 Hz immediately after stimulus onset in control sessions (***D***) but not in MFC D1DR blockade sessions (***E***). Black lines indicate significance of the correlation coefficient at $p < 0.05$. ***F***, A direct comparison of correlations between control and MFC D1DR sessions revealed that correlations between ramping activity and spike-field coherence were stronger only at 4 Hz triggered by the stimulus. ***G***, These data indicate that in control sessions (blue), low-frequency oscillations are observed in MFC neurons, many of which have ramping patterns of activity. In sessions with MFC D1DR blockade (red), low-frequency oscillations, coupling, and ramping activity are attenuated. Our data suggest that ramping neurons could be coherent with stimulus-triggered 4 Hz oscillations but that MFC D1DR blockade attenuated spike-field coherence and changed how spike-field coherence was linked with MFC ramping activity.

MFC D1DR blockade attenuates ramping-related spike-field coherence

If low-frequency oscillations influenced neuronal activity, then these oscillations should exhibit functional coupling with neuronal activity. To test this idea, we examined the coherence between neuronal activity and MFC field potentials (Rosenberg et al., 1989; Narayanan et al., 2013) in the same rodents and recording sessions as described in Materials and Methods. This measure correlates neuronal activity in the frequency domain between LFPs and neuronal activity. In control sessions, across all 99 neurons from nine animals, weak 2–4 Hz spike-field coherence was observed ~500 ms after onset of the stimuli (Fig. 9*A*). However, in sessions with MFC D1DR blockade (Fig. 9*B*), across all 91 neurons in nine animals, significantly less spike-field coherence was observed between 2 and 4 Hz and at 7 Hz than in control sessions (Fig. 9*C*). No differences were seen at higher frequencies. This analysis suggests that, on average, MFC D1DR blockade could attenuate functional coupling of single neurons with these low-frequency oscillations.

To investigate whether ramping neurons were more likely to be coherent with low-frequency oscillations, we examined the relationship between ramping activity as measured by PC1 and spike-field coherence by linear correlation. We found a strong relationship only at stimulus onset between PC1 and spike-field coherence near 4 Hz (Fig. 9*D*). A direct comparison of control and MFC D1DR blockade sessions indicated ramping neurons were more likely to be coherent with 4 Hz oscillations ($r = 0.26$ of spike-field coherence 0–250 ms, 3–5 Hz vs PC1; $t_{(97)} = 2.7$, $p < 0.005$). In sessions with MFC D1DR blockade that decreased ramping activity, this relationship was altered (Fig. 9*E*; $r = -0.13$, $t_{(189)} = 1.2$, $p < 0.11$), and correlation coefficients were significantly different in control and MFC D1DR blockade sessions (Fig. 9*F*; comparing 3–5 Hz correlations for control and MFC D1DR blockade sessions; Fisher's r to $z = 2.7$, $p > 0.004$). These relationships were not observed for higher components. No differences were seen at higher frequencies. Together, these data suggest that neurons ramping down tended to be coherent with low-frequency oscillations around 4 Hz and that both average spike-field coherence and correlations of coherence and ramping activity were altered by MFC D1DR blockade (Fig. 9*G*).

Discussion

In the present study, we tested the hypothesis that MFC D1DR dopamine signaling is necessary for ramping neuronal activity underlying accurate interval timing. We report three novel findings. First, rodents had stimulus-triggered 4–7 Hz oscillations in MFC during interval timing. Second, focal blockade of the D_1 dopamine receptor within the MFC attenuated these oscillations. Finally, MFC D1DR blockade decreased MFC ramping activity linked with behavior and ~4 Hz oscillations. Together, our findings provide novel evidence that MFC D1DR signaling is necessary for neuronal activity during interval timing and sheds light on the mechanism of how neuronal networks organize behavior in time.

In MFC, 4 Hz oscillations were triggered by the discriminative stimulus during interval timing tasks. A review of this effect consistently implicates low frequencies around 4 Hz in stimulus-triggered oscillations in rodents and spike-field coherence, although other frequencies are involved (Table 1). This specific frequency band has been consistently implicated in action monitoring in both humans and rodents (Cavanagh et al., 2012; Narayanan et al., 2013). The 4 Hz oscillations have been specifically linked to synchronizing hippocampal ensembles (Fujisawa and Buzsáki, 2011) with frontal and subcortical nuclei. The slow dynamics of low-frequency oscillations in the present study, and extensive data on such patterns of neuronal activity (Cavanagh et al., 2012), suggest that this signal does not encode stimulus-related attention alone. Notably, MFC dopamine is likely to be released at stimulus onset and may encode time. MFC dopamine has slow dynamics over several seconds (Garris and Wightman, 1994), perhaps accounting for D_1-dependent, low-frequency oscillations increasing several hundred milliseconds after onset of stimuli. The time course of this process is distinct from stimulus-related processing in our data and in previous work in frontal regions (Niki and Watanabe, 1979; Narayanan and Laubach, 2009a) that was independent of D_1 signaling.

We did find evidence that higher frequencies such as beta oscillations were involved in interval timing and influenced by D1DR blockade (Table 1). Although this band was not coherent with single neurons, higher-frequency oscillations have been implicated in cortical interactions with subcortical nuclei and in motor control (Mallet et al., 2008).

MFC D1DR blockade diminished stimulus-related ~4 Hz oscillations. To our knowledge, this is the first report that D_1 blockade diminished these oscillations, although a recent report found that L-dopa increased 4–12 Hz oscillations in frontal cortex (Eckart et al., 2014). D_1 blockade also decreased coupling of ~4 Hz oscillations with neurons that tended to have strong ramping patterns. Although this might be expected from an overall decrease in low-frequency oscillations, these data suggest that without D_1 signaling, ramping neurons are functionally "uncoupled" from a signal encoding the start of the interval. Without this initiating signal, single neurons in MFC do not ramp yet continue to encode other variables such as stimuli and motor parameters (Narayanan and Laubach, 2006). One possible mechanism for these patterns may be that stimulus-triggered dopamine release in MFC facilitates 4 Hz oscillations, which initiates ramping activity of single neurons (Fig. 7*G*). Low-frequency oscillations can synchronize MFC activity with midbrain dopamine neurons as well as the hippocampus (Fujisawa and Buzsáki, 2011). Low-frequency oscillations in our task are not predictive of subsequent behavior (Fig. 8); rather, they tend to be coherent with ramping activity, which in turn predicts timing behavior (Fig. 9). With MFC D1DR blockade, ~4 Hz oscillations, ramping activity, and spike-field coherence are all decreased.

Table 1. Stimulus-triggered oscillations during interval timing

Figure	Signal	Contrast	Frequencies
3*B*	MFC LFP	Interval timing vs baseline	3–7 Hz, 13–46 Hz
5*C*	MFC LFP	Control vs MFC D1DR blockade	3–46 Hz
9*C*	Spike-field coherence	Control vs MFC D1DR blockade	2–4 Hz, 7 Hz
9*D*	Correlation	PC1 vs spike-field coherence	2–4 Hz
9*F*	PC1 vs spike-field coherence correlation	Control vs MFC D1DR blockade	4 Hz

A large body of literature has demonstrated that ramping activity in single neurons is correlated with temporal control of action in timing and reaction time tasks (Durstewitz, 2003; Narayanan and Laubach, 2009a; Kim et al., 2013; Xu et al., 2014). The ramping modulation reported here is in the range of temporal modulations reported in prior work (Matell et al., 2003; Narayanan and Laubach, 2009a; Kim et al., 2013; Xu et al., 2014). Neural activity that follows this pattern can function as an "integrator" (Durstewitz, 2003; Bekolay et al., 2014) and serve as the memory trace in the scalar timing theory (Staddon, 2005). Because ramping activity has been well described in the past, we elected to use a single interval in the present study to increase statistical power. Future studies may extrapolate to an interval timing task with multiple intervals to examine temporal discounting functions; indeed, the influence of dopamine should diminish at longer delays (Fiorillo et al., 2008; Kobayashi and Schultz, 2008).

Our work extends the seminal findings of Goldman-Rakic and colleagues (Williams and Goldman-Rakic, 1995; Goldman-Rakic et al., 2000), who linked D_1 signaling to executive processes such as working memory. Recent work has linked MFC D1DRs with impulsivity (Koffarnus et al., 2011; Pardey et al., 2013). Here we find inhibiting MFC D1DRs causes responses to occur earlier in timing tasks and decreases ramping activity that has been linked with inhibiting responses until a temporal "deadline," after which responses lead to rewards (Ollman and Billington, 1972; Narayanan et al., 2006; Smith et al., 2010). Our data provide insight into how dopamine signaling affects medial frontal neuron activity to powerfully influence the temporal organization of behavior. These data may be developed into biomarkers for MFC dysfunction in ADHD, schizophrenia, Parkinson's disease, and other diseases involving dopamine.

References

Allen TA, Narayanan NS, Kholodar-Smith DB, Zhao Y, Laubach M, Brown TH (2008) Imaging the spread of reversible brain inactivations using fluorescent muscimol. J Neurosci Methods 171:30–38. CrossRef Medline

Balci F, Papachristos EB, Gallistel CR, Brunner D, Gibson J, Shumyatsky GP (2008) Interval timing in genetically modified mice: a simple paradigm. Genes Brain Behav 7:373–384. CrossRef Medline

Bekolay T, Laubach M, Eliasmith C (2014) A spiking neural integrator model of the adaptive control of action by the medial prefrontal cortex. J Neurosci 34:1892–1902. CrossRef Medline

Buhusi CV, Meck WH (2005) What makes us tick? Functional and neural mechanisms of interval timing. Nat Rev Neurosci 6:755–765. CrossRef Medline

Caetano MS, Church RM (2009) A comparison of responses and stimuli as time markers. Behav Processes 81:298–302. CrossRef Medline

Cavanagh JF, Cohen MX, Allen JJ (2009) Prelude to and resolution of an error: EEG phase synchrony reveals cognitive control dynamics during action monitoring. J Neurosci 29:98–105. CrossRef Medline

Cavanagh JF, Figueroa CM, Cohen MX, Frank MJ (2012) Frontal theta reflects uncertainty and unexpectedness during exploration and exploitation. Cereb Cortex 22:2575–2586. CrossRef Medline

Chapin JK, Nicolelis MA (1999) Principal component analysis of neuronal

ensemble activity reveals multidimensional somatosensory representations. J Neurosci Methods 94:121–140. CrossRef Medline
Church R (2003) A concise introduction to scalar timing theory. In: Functional and neural mechanisms of interval timing (Meck W, ed), pp 3–22. Boca Raton, FL: CRC. CrossRef
Church RM (1984) Properties of the internal clock. Ann N Y Acad Sci 423: 566–582. CrossRef Medline
Cools R, D'Esposito M (2011) Inverted-U-shaped dopamine actions on human working memory and cognitive control. Biol Psychiatry 69:e113–e125. CrossRef Medline
Coull JT, Cheng RK, Meck WH (2011) Neuroanatomical and neurochemical substrates of timing. Neuropsychopharmacology 36:3–25. CrossRef Medline
Durstewitz D (2003) Self-organizing neural integrator predicts interval times through climbing activity. J Neurosci 23:5342–5353. Medline
Eckart C, Fuentemilla L, Bauch EM, Bunzeck N (2014) Dopaminergic stimulation facilitates working memory and differentially affects prefrontal low theta oscillations. Neuroimage 94:185–192. CrossRef Medline
Fiorillo CD, Newsome WT, Schultz W (2008) The temporal precision of reward prediction in dopamine neurons. Nat Neurosci 11:966–973. CrossRef Medline
Fry W, Kelleher RT, Cook L (1960) A mathematical index of performance on fixed-interval schedules of reinforcement. J Exp Anal Behav 3:193–199. CrossRef Medline
Fujisawa S, Buzsáki G (2011) A 4 Hz oscillation adaptively synchronizes prefrontal, VTA, and hippocampal activities. Neuron 72:153–165. CrossRef Medline
Garris PA, Wightman RM (1994) Different kinetics govern dopaminergic transmission in the amygdala, prefrontal cortex, and striatum: an in vivo voltammetric study. J Neurosci 14:442–450. Medline
Gibbon J, Church RM, Meck WH (1984) Scalar timing in memory. Ann N Y Acad Sci 423:52–77. CrossRef
Goldman-Rakic PS, Muly EC 3rd, Williams GV (2000) D(1) receptors in prefrontal cells and circuits. Brain Res Brain Res Rev 31:295–301. CrossRef Medline
Hyman JM, Whitman J, Emberly E, Woodward TS, Seamans JK (2012) Action and outcome activity state patterns in the anterior cingulate cortex. Cereb Cortex 23:1257–1268. CrossRef Medline
Jahanshahi M, Jones CR, Zijlmans J, Katzenschlager R, Lee L, Quinn N, Frith CD, Lees AJ (2010) Dopaminergic modulation of striato-frontal connectivity during motor timing in Parkinson's disease. Brain 133:727–745. CrossRef Medline
Kim J, Jung AH, Byun J, Jo S, Jung MW (2009) Inactivation of medial prefrontal cottex impairs time interval discrimination in rats. Front Behav Neurosci 3:38. CrossRef Medline
Kim J, Ghim JW, Lee JH, Jung MW (2013) Neural correlates of interval timing in rodent prefrontal cortex. J Neurosci 33:13834–13847. CrossRef Medline
Kobayashi S, Schultz W (2008) Influence of reward delays on responses of dopamine neurons. J Neurosci 28:7837–7846. CrossRef Medline
Koffarnus MN, Newman AH, Grundt P, Rice KC, Woods JH (2011) Effects of selective dopaminergic compounds on a delay-discounting task. Behav Pharmacol 22:300–311. CrossRef Medline
Krupa DJ, Wiest MC, Shuler MG, Laubach M, Nicolelis MA (2004) Layer-specific somatosensory cortical activation during active tactile discrimination. Science 304:1989–1992. CrossRef Medline
Ma L, Hyman JM, Phillips AG, Seamans JK (2014) Tracking progress toward a goal in corticostriatal ensembles. J Neurosci 34:2244–2253. CrossRef Medline
Malapani C, Rakitin B, Levy R, Meck WH, Deweer B, Dubois B, Gibbon J (1998) Coupled temporal memories in Parkinson's disease: a dopamine-related dysfunction. J Cogn Neurosci 10:316–331. CrossRef Medline
Mallet N, Pogosyan A, Sharott A, Csicsvari J, Bolam JP, Brown P, Magill PJ (2008) Disrupted dopamine transmission and the emergence of exaggerated beta oscillations in subthalamic nucleus and cerebral cortex. J Neurosci 28:4795–4806. CrossRef Medline
Martin JH, Ghez C (1993) Differential impairments in reaching and grasping produced by local inactivation within the forelimb representation of the motor cortex in the cat. Exp Brain Res 94:429–443. Medline
Matell MS, Meck WH, Nicolelis MA (2003) Interval timing and the encoding of signal duration by ensembles of cortical and striatal neurons. Behav Neurosci 117:760–773. CrossRef Medline
Mauk MD, Buonomano DV (2004) The neural basis of temporal processing. Annu Rev Neurosci 27:307–340. CrossRef Medline
Myers RD (1966) Injection of solutions into cerebral tissue: relation between volume and diffusion. Physiol Behav 1:171–174, IN9. CrossRef
Narayanan NS, Laubach M (2006) Top-down control of motor cortex ensembles by dorsomedial prefrontal cortex. Neuron 52:921–931. CrossRef Medline
Narayanan NS, Laubach M (2008) Neuronal correlates of post-error slowing in the rat dorsomedial prefrontal cortex. J Neurophysiol 100:520–525. CrossRef Medline
Narayanan NS, Laubach M (2009a) Delay activity in rodent frontal cortex during a simple reaction time task. J Neurophysiol 101:2859–2871. CrossRef Medline
Narayanan NS, Laubach M (2009b) Methods for studying functional interactions among neuronal populations. Methods Mol Biol 489:135–165. CrossRef Medline
Narayanan NS, Horst NK, Laubach M (2006) Reversible inactivations of rat medial prefrontal cortex impair the ability to wait for a stimulus. Neuroscience 139:865–876. CrossRef Medline
Narayanan NS, Land BB, Solder JE, Deisseroth K, DiLeone RJ (2012) Prefrontal D1 dopamine signaling is required for temporal control. Proc Natl Acad Sci U S A 109:20726–20731. CrossRef Medline
Narayanan NS, Cavanagh JF, Frank MJ, Laubach M (2013) Common medial frontal mechanisms of adaptive control in humans and rodents. Nat Neurosci 16(12):1888–1895. CrossRef
Niki H, Watanabe M (1979) Prefrontal and cingulate unit activity during timing behavior in the monkey. Brain Res 171:213–224. CrossRef Medline
Ollman RT, Billington MJ (1972) The deadline model for simple reaction times. Cogn Psychol 3:311–336. CrossRef
Pardey MC, Kumar NN, Goodchild AK, Cornish JL (2013) Catecholamine receptors differentially mediate impulsive choice in the medial prefrontal and orbitofrontal cortex. J Psychopharmacol (Oxford) 27:203–212. CrossRef
Parker KL, Alberico SL, Miller AD, Narayanan NS (2013a) Prefrontal D1 dopamine signaling is necessary for temporal expectation during reaction time performance. Neuroscience 255:246–254. CrossRef Medline
Parker KL, Lamichhane D, Caetano MS, Narayanan NS (2013b) Executive dysfunction in Parkinson's disease and timing deficits. Front Integr Neurosci 7:75. CrossRef Medline
Paz R, Natan C, Boraud T, Bergman H, Vaadia E (2005) Emerging patterns of neuronal responses in supplementary and primary motor areas during sensorimotor adaptation. J Neurosci 25:10941–10951. CrossRef Medline
Rakitin BC, Gibbon J, Penney TB, Malapani C, Hinton SC, Meck WH (1998) Scalar expectancy theory and peak-interval timing in humans. J Exp Psychol Anim Behav Process 24:15–33. CrossRef Medline
Rosenberg JR, Amjad AM, Breeze P, Brillinger DR, Halliday DM (1989) The Fourier approach to the identification of functional coupling between neuronal spike trains. Prog Biophys Mol Biol 53:1–31. CrossRef Medline
Sawaguchi T, Goldman-Rakic PS (1994) The role of D1-dopamine receptor in working memory: local injections of dopamine antagonists into the prefrontal cortex of rhesus monkeys performing an oculomotor delayed-response task. J Neurophysiol 71:515–528. Medline
Sheth SA, Mian MK, Patel SR, Asaad WF, Williams ZM, Dougherty DD, Bush G, Eskandar EN (2012) Human dorsal anterior cingulate cortex neurons mediate ongoing behavioural adaptation. Nature 488:218–221. CrossRef Medline
Simen P, Balci F, de Souza L, Cohen JD, Holmes P (2011) A model of interval timing by neural integration. J Neurosci 31:9238–9253. CrossRef Medline
Smith NJ, Horst NK, Liu B, Caetano MS, Laubach M (2010) Reversible inactivation of rat premotor cortex impairs temporal preparation, but not inhibitory control, during simple reaction-time performance. Front Integr Neurosci 4:124. CrossRef Medline
Staddon JER (2005) Interval timing: memory, not a clock. Trends Cogn Sci 9:312–314. CrossRef Medline
Taylor KM, Horvitz JC, Balsam PD (2007) Amphetamine affects the start of responding in the peak interval timing task. Behav Processes 74:168–175. CrossRef Medline
Williams GV, Goldman-Rakic PS (1995) Modulation of memory fields by dopamine D1 receptors in prefrontal cortex. Nature 376:572–575. CrossRef Medline
Xu M, Zhang SY, Dan Y, Poo MM (2014) Representation of interval timing by temporally scalable firing patterns in rat prefrontal cortex. Proc Natl Acad Sci U S A 111:480–485. CrossRef Medline